The Accuracy of Characteristic Length Method on Failure Load Prediction of Composite Pinned Joints

O. Aluko, and Q. Mazumder

Abstract— **An analytical model was developed to investigate the choice of failure criterion based on characteristic length method for predicting composite joint strength. The available experimental data for joint strength in literature were used to determine the accuracy of analytically obtained results. The analysis utilized six failure criteria, where it was shown that among the failure criteria investigated no one gave a best fit for all the three plates evaluated for strength, and the fit of individual failure theories is variable from one type of material to another. The results also showed that the accuracy of this method can be improved by computing the average predicted values of more than three failure criteria.**

Index Terms— **Characteristic length, Composite, Failure Criteria, and Joint strength .**

I. Introduction

Adhesive bonding and mechanical bonding remain the two most common methods of joint design. While an adhesive joint offers the advantage of distributing the load over a larger area than a mechanical joint, its use is very restrictive due to its sensitivity to environmental conditions such as temperature and humidity. Therefore, mechanical joints are widely used as a reliable and practical method to assemble the composite parts that constitute a mechanical structure; they offer the advantage of assembly and disassembly for accessibility and maintenance, and reliability at various environmental conditions. However, a significant drawback when using the mechanical joint is that it always requires joint holes, which can be a source of stress concentration and thereby weakens the intended strength for the structures. Therefore, for the design of composite joints, stress and failure analysis around the fastener hole should first be conducted.

During the loading of mechanical joints, the laminate deforms as the applied load increases and the contact surface between the fastener and the plate changes. It should be noted that despite the fact that the distributed stress around the fastener hole could be accurately determined, the failure at any point within the stress concentration region does not necessarily lead to failure of the joints. The strength of the structure will be underestimated if local failure is taken to be the ultimate failure of the joint. It becomes a big task to develop an analytic or computational method that can adequately model the complicated failure and structural response to loading of composite joints. Because of the complexity of the failure of composite joints coupled with the intension to reduce the cost and materials wastage in practical testing to failure, the analytical determination of bolted joint strength has received the attention of many researchers [1]-[16].

One of the most common and efficient methods of predicting the strength is the characteristic length method. This method was proposed by Whiney and Nuismer [1]-[3], and it has been further developed by Chang et. al [4]. For this improved method, both the characteristic lengths in tension, R_t, and compression, R_c, must be determined by stress analysis associated with the results of bearing and tensile tests on notched and unnotched plates before employing an appropriate failure theory along the characteristic curve, r_c as shown in Figure 1. By definition, the characteristic length (in tension or compression) is the radial distance from the hole boundary over which the plate must be critically stressed to initiate a sufficient flaw that can cause failure.

Wang et al. [5] analytically determined failure strength of composite joints in both circular and elliptical holes using stress functions developed by Lehknitskii [6] and Tsai-Wu failure criterion. However, only characteristic length in tension was used around the hole boundary to evaluate the failure load and mode of the composite joint. Whitworth et al. [7], [8] utilized the characteristic curve developed by Chang et. al [4] (which requires both the characteristic length in tension and compression to be determined) along with Yamada failure criterion to evaluate joint strength.

Kweon et al. [9] developed a new method for finding the characteristic length in terms of arbitrarily applied loads, as an alternative to the failure load of notched plate in tension and bearing load of the plate when in compression. They evaluated the joint strength along the characteristic curve using Tsai-Wu failure criterion.

In spite of the significant effort that has been invested on strength estimation of composite joints by various investigators using characteristic length method, the choice of an effective failure criterion in order to improve the accuracy of the characteristic dimensions remains to be investigated. For this paper, various failure criteria were utilized with the characteristic length method to predict the strength of composite joints with the objective to optimize the prediction accuracy of the characteristic length method. A two-dimensional analysis which utilized stress functions for the computation of stresses at the hole boundary and within the plate was employed. In this investigation of the effective choice of failure criterion on the prediction accuracy of joint strength, six selected failure criteria based on the previous survey by Nahas [10] were utilized.

Manuscript submitted March 2, 2010. The Accuracy of Characteristic Length Method on Failure Load Prediction of Composite Pinned Joints.

Olanrewaju Aluko is with the University of Michigan-Flint, 303 E. Kearsley Street, Flint, MI 48502 USA (phone: 810-762-3181; fax: 810-766-6780; e-mail: aluko@ umflint.edu).

Quamrul Mazumder., is with University of Michigan-Flint, 303 E. Kearsley Street, Flint, MI 48502, USA. (e-mail: qmazumde@umflint.edu)..

II. CHARACTERICTIC LENGTHS METHOD

As stated earlier, one of the most common and efficient methods of predicting joint strength is the characteristic length method. This study utilized the characteristic curve first proposed by Chang et al. [4], which requires both the characteristics length in tension, R_t and compression, R_c. These must be determined by stress analysis associated with the results of no-bearing and tensile tests on notched and unnotched plates before employing an appropriate failure theory along the characteristic curve, r_c as shown in Fig. 1. This characteristic curve which can be expressed as:

$$r_c = d/2 + R_t + (R_t - R_c)\cos\theta \quad (1)$$

where x and y are equal to $r_c\cos\theta$ and $r_c\sin\theta$ respectively.

In this study, the plate (MO1) made from carbon-epoxy unidirectional prepreg (USN125) and plain weave prepreg (HPW193) [11] with stacking sequence $[\pm45_3/90/\pm45_2/0_4/90/0_4//\pm45_2/90/\pm45_3]$ was used. The notation "±45" is used to represent a plane weave carbon/epoxy layer and the lamina thicknesses of the unidirectional and woven fabric layers are 0.125 mm and 0.19 mm respectively. The hole diameter (d) is 9.53 mm, the width (W) of the plate is 26.8 mm, and the edge distance (e) is 19 mm. MO2 composite plate [9] was also utilized, having the same stacking sequence as above. The unidirectional layers are from the USN125 graphite/epoxy prepreg by Hankook Fiber Glass. The DMS2288 graphite/epoxy woven fabrics are by Sunkyong. The one-ply-thicknesses of the unidirectional and woven fabric layers are 0.114 mm and 0.198 mm, respectively. Other geometries of these two plates are the same. Additionally, AS4/3501-6 graphite/epoxy laminate having the stacking sequence $[(45/0/-45/0/90/0/45/0/-45/0)_2]_s$ with geometry of diameter (d), thickness (h), ratio of end distance to hole diameter (e/d) equal to 0.635 cm, 0.584 cm and 2, respectively was also used in this analysis [7]. The material properties of the three laminates are as given in Table I.

a) Compressive characteristic length

This analytical method employs the new approach proposed by Kweon et al. [9], without bearing tests to evaluate characteristic length in compression. This method utilizes any arbitrary load to compute the mean bearing stress, defined by:

$$\sigma_{mb} = {P_m}/{dh} \quad (2)$$

where, P_m, d and h are the arbitrary loads, diameter of hole and laminate thickness respectively. Within the context of this

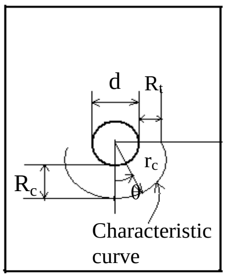

Fig. 1. Schematic diagram for characteristic curve

method, the compressive characteristic length R_c as showed in Fig. 2 for point stress criterion [1] is the distance from the front hole-edge to a point where the local compressive stress by the arbitrarily applied load is the same as the mean bearing stress.

The present study utilized an analytical technique proposed by Aluko [12] to determine the compressive characteristic length. The analysis involved the stress functions that were computed from the displacement expressions that satisfy the boundary conditions. The semi-infinite plate in compression is as shown in Fig. 3.

The boundary conditions of this geometry can be expressed as:

$$u = u_o \text{ and } v = 0 \quad at\ \theta = \pm{\pi}/{2} \quad (3)$$

$$u = {u_0}/{c} \text{ and } v = 0 \quad at\ \theta = 0 \quad (4)$$

$$(u_o - u)\cos\theta = v\sin\theta \text{ between} -{\pi}/{2} \le \theta \le {\pi}/{2} \quad (5)$$

where *u* and *v* are the displacements along x and y axes respectively.

Therefore, the displacements *u* and *v* along the hole can be expressed by the following trigonometric series,

$$u = u_1\cos2\theta + u_2\cos4\theta \quad (6)$$

$$v = v_1\sin2\theta + v_2\sin4\theta \quad (7)$$

where u_1, u_2, v_1 and v_2 are the unknowns to determine from boundary conditions.

The condition of at free surface where x equal zero is:

$$\sigma_x = 0 \text{ and } \tau_{xy} = 0 \quad (8)$$

Substituting (6) and (7) into (3), (4) and (5), we have

Table I. The material properties of composite materials

Properties	Type of Material			
	USN 125	HPW 193	DMS 2288	AS43501-6
E_1 (GPa)	131	65.4	65	144.14
E_2 (GPa)	8.2	65.4	65	11.72
G_{12} (GPa)	4.5	3.59	3.6	6.69
υ_{12}	0.281	0.058	0.058	0.33
X_c (MPa)	1400	692.9	692.9	1480
X_t (MPa)	2000	959.1	959	1860
Y_c (MPa)	130	692.9	692.9	210
Y_t (MPa)	61	959.1	959	50
S_{12} (MPa)	70	64.9	65	60

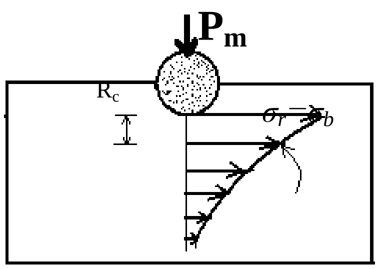

Fig. 2. Schematic diagram of the compressive characteristic length and normal stress distribution pattern

ISBN: 978-988-18210-7-2
ISSN: 2078-0958 (Print); ISSN: 2078-0966 (Online)

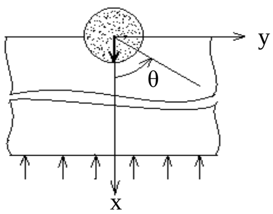

Fig. 3. Schematic representation of compressive loading

$$u_1 = {}^{(c-1)u_o}/_{2c}, u_2 = v_2 = {}^{(c+1)u_o}/_{2c} \text{ and } v_1 = {}^{(3c+1)u_o}/_{2c} \tag{9}$$

The stress functions that satisfy the above displacement boundary conditions are [6]:

$$\emptyset_1(z_1) = A\ln\varsigma_1 + ({}^1/_{2D})[(u_1q_2 - iv_1p_2)\varsigma_1^{-2} + (u_2q_2 - iv_2p_2)\,\varsigma_1^{-2}] \tag{10}$$

$$\emptyset_2(z_2) = B\ln\varsigma_2 + ({}^1/_{2D})[(u_1q_1 - iv_1p_1)\varsigma_2^{-2} + (u_2q_1 - iv_2p_1)\,\varsigma_2^{-2}] \tag{11}$$

However, the stresses in rectangular co-ordinate can be expressed as:

$$\sigma_x = 2Re\{\mu_1{}^2\emptyset_1'(z_1) + (\mu_2{}^2\emptyset_2'(z_2)\}$$
$$\tau_{xy} = -2Re\{(\mu_1\emptyset_1'(z_1) + \mu_2\emptyset_2'(z_2) \tag{12}$$
$$\sigma_y = 2Re\{\emptyset_1'(z_1) + \emptyset_2'(z_2)\}$$

Further, the stresses in polar co-ordinates can be obtained by stress transformations.

In this model, frictionless condition is assumed between the pin and plate, Therefore, constant u_o and c can be obtained from:

$$\tau_{r\theta} = 0 \qquad \text{at } \theta = \pm\pi/2 \tag{13}$$

$$\int_0^{\frac{\pi}{2}} \tau_{r\theta}\, r\, d\theta = 0 \tag{14}$$

b) Tensile characteristic length

Joints evaluation by the characteristic length method also requires the determination of tensile characteristic length. This involves the tensile test of notched (σ_{no}) and unnotched (σ_{un}) laminate, as the strength values for the notched and unnotched laminates in tension must be known a priori. Fig. 4 shows the stress distribution of an infinite plate with a through-to-thickness hole subjected to distributed tensile loads per unit area, P at infinity. The tensile stress would be highest at the side edges of the hole, and decreases further away from the side edges of the hole as shown in Fig. 4.

In this analysis, the idea proposed by Konish and Whitney [13] for the approximate solution to the normal stress distribution σ_y (x,0) in an infinite orthotropic plate with an open hole loaded in tension would be utilized. This solution can be expressed as:

$$\frac{\sigma_y(x,0)}{P} \cong 1 + \frac{1}{2}\xi^{-2} + \frac{3}{2}\xi^{-4} - \frac{(K_T^\infty - 3)}{2}(5\xi^{-6} - 7\xi^{-8}) \tag{15}$$

where the stress concentration factor K^∞_T and ξ are expressed by the following:

$$K_T^\infty = 1 + \sqrt{\frac{2}{A_{22}}\left(\sqrt{(A_{11}A_{22})} - A_{12} + \frac{A_{11}A_{22} - A_{12}^2}{2A_{66}}\right)} \tag{16}$$

$$\xi = \frac{x}{r} \tag{17}$$

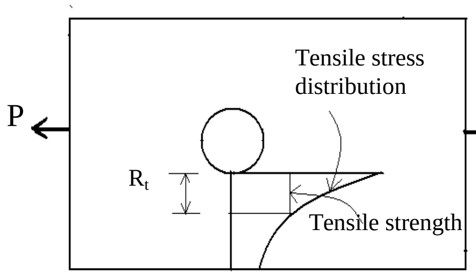

Fig. 4. Schematic diagram of the tensile characteristic length and stress distribution pattern

where A_{ij}, i,j = 1,2,6 denote the effective laminate in-plane stiffness with 1 and 2 parallel and perpendicular to the loading direction respectively.

The point stress criterion [2] can be applied to (15) to compute the tensile characteristic length at which failure analysis of the joint should be evaluated. The criterion defines the tensile characteristic length as the distance from the side-edge of the hole to a point where the tensile stress is the same as the strength of unnotched laminate. This can be expressed as:

$$\sigma_y(x,0) = \sigma_{un} \tag{18}$$

where,

$$x = r + R_t;\ P = \sigma_{no} \tag{19}$$

The criterion assumes that the stress at infinity that determines the characteristic length defines the strength of the notched laminate. Substituting (17) and (18) into (15), the ratio of unnotched to notched strength is obtained as:

$$\frac{\sigma_{un}}{\sigma_{no}} = 1 + \frac{1}{2}\xi^{-2} + \frac{3}{2}\xi^{-4} - \frac{(K_T^\infty - 3)}{2}(5\xi^{-6} - 7\xi^{-8}) \tag{20}$$

The value of tensile characteristic length can be determined if the data for tensile notched and unnotched laminate strength are known. The experimental values of notched and unnotched strength as obtained in the literature and the calculated values of both compressive and tensile characteristic length are shown in Table II.

III. JOINT STRENGTH AND FAILURE ANALYSIS

The present approach utilized an analytical technique that considers the orthotropic plate loaded with a force P by a rigid and frictionless pin (as shown in Fig. 5) to be homogeneous and infinite. In addition, the pin has the same diameter as the circular hole in the plate. Let the displacement of the plate due to pin load along x axis and at the ends of contact boundary be c_o and c_1, respectively. Therefore, the boundary conditions of the geometry shown in Fig. 5 can be expressed as follows:

$$u = c_o \text{ and } v = 0 \qquad at\ \theta = 0 \tag{21}$$

Table II: Characteristic length and strength data for the plates

Plate	R_c, m	R_t, m	Notched strength, MPa	Unnotched strength, MPa
MO1	0.00132	0.004296	703.69	880.00
MO2	0.00347	0.006850	793.00	874.00
AS43501-6	0.00125	0.000845	376.00	695.00

ISBN: 978-988-18210-7-2
ISSN: 2078-0958 (Print); ISSN: 2078-0966 (Online)

$$u = c_1 \text{ and } v = 0 \quad \text{at } \theta = {}^{3\pi}/_2,\ {}^{\pi}/_2 \tag{22}$$
$$c_o = u + v\tan\theta \tag{23}$$
where *u* and *v* are the displacements along x and y axes respectively.
The condition for no contact surface can be expressed as:
$$\sigma_r = 0 \tag{24}$$
$$\tau_{r\theta} = 0 \tag{25}$$
Using (6) and (7) to satisfy the above displacement boundary conditions, we calculated the unknown u_i and v_i to be:
$$u_1 = {}^{(c_o - c_1)}/_2,\ u_2 = {}^{(c_o + c_1)}/_2 \tag{26a}$$
$$v_2 = {}^{(c_o + c_1)}/_2 \text{ and } v_1 = {}^{(3co + c_1)}/_2 \tag{26b}$$
The stress functions that satisfy the above displacement boundary conditions are [6]:
$$\emptyset_1(z_1) = A\ln\varsigma_1 + \left({}^1/_{4D}\right)[((c_o - c_1)q_2 - i(3co + c_1)p_2)\varsigma_1^{-2} + ((c_o + c_1)q_2 - i(c_o + c_1)p_2)\,\varsigma_1^{-2}] \tag{27a}$$
$$\emptyset_2(z_2) = B\ln\varsigma_2 - \left({}^1/_{4D}\right)[((c_o - c_1)q_1 - i(3co + c_1p_1)\varsigma_2^{-2} - ((c_o + c_1)q_1 - i(c_o + c_1)p_1)\,\varsigma_2^{-2}] \tag{27b}$$

The stresses in rectangular co-ordinates can be expressed as [6]:
$$\sigma_x = 2\mathrm{Re}\{\mu_1{}^2\emptyset_1'(z_1) + (\mu_2{}^2\emptyset_2'(z_2)\} \tag{28a}$$
$$\tau_{xy} = -2\mathrm{Re}\{(\mu_1\emptyset_1'(z_1) + \mu_2\emptyset_2'(z_2)\} \tag{28b}$$
$$\sigma_y = 2\mathrm{Re}\{\emptyset_1'(z_1) + \emptyset_2'(z_2)\} \tag{28c}$$
$$A = \left({}^P/_{\pi hi}\right)\left(\mu_1\bar{\mu}_1 + \mu_1\mu_2 + \mu_1\bar{\mu}_2 - \left({}^{a_{12}}/_{a_{22}}\right)\mu_1\mu_2\bar{\mu}_1\bar{\mu}_2\right)/ ((\mu_1 - \bar{\mu}_1)(\mu_1 - \mu_2)(\mu_1 - \bar{\mu}_2)) \tag{29}$$
$$B = \left({}^P/_{\pi hi}\right)\left(\mu_2\bar{\mu}_2 + \mu_1\mu_2 + \mu_2\bar{\mu}_1 - \left({}^{a_{12}}/_{a_{22}}\right)\mu_1\mu_2\bar{\mu}_1\bar{\mu}_2\right)/ ((\mu_2 - \bar{\mu}_2)(\mu_2 - \mu_1)(\mu_2 - \bar{\mu}_1)) \tag{30}$$

where bar implies conjugate and
$$p_1 = a_{11}\mu_1{}^2 + a_{12} \text{ and } p_2 = a_{11}\mu_2{}^2 + a_{12} \tag{31}$$
$$q_1 = a_{12}\mu_1 + {}^{a_{22}}/_{\mu_1} \text{ and } q_2 = a_{12}\mu_2 + {}^{a_{22}}/_{\mu_2} \tag{32}$$
$$\varsigma_k = \left(z_k \pm \sqrt{z_k^2 - \mu_k^2 r^2 - r^2}\right)/(r - i\mu_k r) \qquad k = 1,2 \tag{33}$$
with a_{ij}, *i,j =1,2,6* are the compliances, and μ_1 and μ_2 are the roots of characteristics equation for orthotropic plate defined by:
$$a_{11}\mu^4 + (2a_{12} + a_{66})\mu^2 + a_{22} = 0 \tag{34}$$
where 1 and 2 are parallel and transverse to the loading direction, respectively, and r is the radius of the hole.
The stresses in polar co-ordinates are given by the expressions:

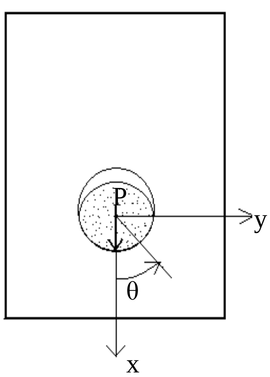

Fig. 5. Schematic representation of composite joint

$$\sigma_r = 2Re\{(\sin\theta - \mu_1\cos\theta)^2\emptyset_1'(z_1) + (\sin\theta - \mu_2\cos\theta)^2\emptyset_2'(z_2)\}$$
$$\tau_{r\theta} = 2Re\{(\sin\theta - \mu_1\cos\theta)(\cos\theta + \mu_1\sin\theta)\emptyset_1'(z_1) + (\sin\theta - \mu_2\cos\theta)(\cos\theta + \mu_2\sin\theta)\emptyset_2'(z_2)\} \tag{35}$$
$$\sigma_\theta = 2Re\{(\mu_1\sin\theta + \cos\theta)^2\emptyset_1'(z_1) + (\mu_2\sin\theta + \cos\theta)^2\emptyset_2'(z_2)\}$$
The prime implies the derivative of the stress functions.
The parameters c_o and c_1 can be determined from material properties of the plate and the condition of traction at the hole boundary. The traction for the case frictionless condition can be expressed as:
$$\tau_{r\theta} = 0 \qquad \text{at } \theta = \pi/2 \tag{36}$$
$$\int_0^{\frac{\pi}{2}} \tau_{r\theta}\, r\, d\theta = 0 \tag{37}$$
$$c_0 = gP(9n + k(10 + 21n) - 10v_{12})/4h\pi(k^2(5 + 13n + 3n^2) + k(12n^2 + n(7 - 13v_{12}) - 10v_{12}) + v_{12}(-7n + 5v_{12})) \tag{38a}$$
$$c_1 = gP(k(-10 - 11n) - 19n + 10v_{12}/4h\pi(k^2(5 + 13n + 3n^2) + k(12n^2 + n(7 - 13v_{12}) - 10v_{12}) + v_{12}(-7n + 5v_{12})) \tag{38b}$$
Parameters k, n and g are materials constant of the plate expressed as:
$$k = -\mu_1\mu_2 = (E_1/E_2)^{1/2}$$
$$n = -i(\mu_1 + \mu_2) = [2(k - v_{12}) + E_1/G_{12}]^{1/2}$$
$$g = (1 - v_{12}v_{21})/E_2 + k/G_{12} \tag{40}$$
The stress results computed from above analytical method along the characteristic curve (shown in Fig. 1) were used in failure analysis to predict the joint strength for first ply failure. In an attempt to increase the accuracy of joint strength prediction by characteristic length method, six failure criteria based on the previous survey by Nahas [10] were used in conjunction with characteristic dimensions for the evaluation. In his survey, Nahas referenced the previous study by Burk [15] stating that Azzi-Tsai and Tsai-Wu are among the four most commonly used failure criteria. Nahas also referenced the work of Owen and Rice [16] that asserts Fischer theory provides the best overall fit for static test results. The various failure criteria utilized in this analysis include the following [10]:

Yamada-Sun: $\left(\frac{\sigma_1}{X}\right)^2 + \left(\frac{\tau_{12}}{S}\right)^2 = 1$ (41)

Azzi-Tsai: $\left(\frac{\sigma_1}{X}\right)^2 - \frac{\sigma_1\sigma_2}{X^2} + \left(\frac{\sigma_2}{Y}\right)^2 + \left(\frac{\tau_{12}}{S}\right)^2 = 1$ (42)

Fisher: $\left(\frac{\sigma_1}{X}\right)^2 + \left(\frac{\sigma_2}{Y}\right)^2 + \left(\frac{\tau_{12}}{S}\right)^2 - \frac{E_1(1+v_{21})+E_2(1+v_{12})}{2\sqrt{E_1E_1(1+v_{21})(1+v_{12})}}\frac{\sigma_1\sigma_2}{XY} = 1$ (43)

Tsai-Wu:
$$F_1\sigma_1 + F_2\sigma_2 + F_{11}\sigma_1^2 + F_{22}\sigma_2^2 + F_{11}\tau_{12}^2 + 2F_{12}\sigma_1\sigma_2 = 1 \tag{44}$$

Norris: $\left(\frac{\sigma_1}{X}\right)^2 - \frac{\sigma_1\sigma_2}{XY} + \left(\frac{\sigma_2}{Y}\right)^2 + \left(\frac{\tau_{12}}{S}\right)^2 = 1$ (45)

Norris-Mckinnon: $\left(\frac{\sigma_1}{X}\right)^2 + \left(\frac{\sigma_2}{Y}\right)^2 + \left(\frac{\tau_{12}}{S}\right)^2 = 1$ (46)

Where σ_1 and σ_2 are longitudinal stresses and τ_{12} is shear stress, X and Y are the ply longitudinal strength and S the ply shear strength. In this model, failure is expected to occur when the above equations are met. The computer code used to test for the condition of failure was written in Mathematica.

The concept of finite-width correction factor developed by Tan [14] was utilized to correct the infinite assumption of the plate. By definition, finite-width correction factor (FWC) is a scale factor which is applied to multiply the notched infinite plate solution to obtain the notched

ISBN: 978-988-18210-7-2
ISSN: 2078-0958 (Print); ISSN: 2078-0966 (Online)

finite-plate result based on the assumption that the normal stress profile for a finite plate is identical to that for an infinite except for a FWC factor. This correction factor is given by the relationship:

$$\frac{K_T^{\infty}}{K_T}\sigma_N^{\infty} = \sigma_N \qquad (47)$$

K_T/K_T^{∞} is the FWC factor and K_T and K_T^{∞} denote the stress concentration at the opening edge on the axis normal to the applied load for a finite plate and an infinite plate, respectively. The parameters σ_N and σ_N^{∞} are the failure strength of finite-width and infinite plates, respectively. This factor is expressed by the relationship [14]:

$$\frac{K_T^{\infty}}{K_T} = \frac{\left[2-\left(\frac{2r}{w}\right)^2-\left(\frac{2r}{w}\right)^4\right]}{2} + \frac{\left(\frac{2r}{w}\right)^6 (K_T^{\infty}-3)\left[1-\left(\frac{2r}{w}\right)\right]}{2} \qquad (48)$$

where r is the radius of the hole and w defines the width of the plate.

IV. RESULTS AND DISCUSSION

The failure loads computed from the above analysis with failure criteria and their percentage differences with the experimentally obtained value for three different composite plates are shown in Table III. It can be seen from this table that no criterion provided the best fit for all the plate evaluated, and the fit of individual failure theories is variable from one type of material to another. Documented in Fig. 6 is the predicted load for MO1 plate as compared with experimental value. Due to variability in material properties, the experimental value for this plate [11] varies between 11.3 and 13.0 kN, which can be approximated to ±7.13% over the mean value. It can be depicted from this figure that all the predictions except Tsai-Wu which over estimated the strength are suitable for this plate.

Keweon et al. [9] showed that seven specimens were tested for plate MO2 and the computed coefficient of variation (defined as standard deviation over the mean failure load) was equal to 6.1 percent. Even though the range for the experimental failure load cannot be computed from the coefficient of variation, it is evident from Fig. 7 that Fisher criterion is not an adequate predictor of strength. Therefore, the conclusion reached by Owen and Rice [16] that the Fisher theory provides the best overall fit for static tests results does not apply to all plates, as shown in this figure. Fisher theory severely underestimated the failure strength for MO2 plate. For AS43501-6 plate, no information with regard to material variability was given. Notwithstanding, all the various criteria employed in this study appear to be adequate for the plate as documented in Fig. 8, with Fisher criterion yielding the best prediction. It should be noted that while Tsai-Wu failure theory over estimates the failure strength for all the three plates evaluated, the calculated average values of each prediction give a better fit for all the plates.

V. CONCLUSION

Stress analysis was performed to predict failure strength of pin loaded composite joints using the six failure criteria and on Chang-Scott-Springer characteristic curve model. The characteristic length in compression and tension that defines the characteristic curve was obtained by stress analysis associated with no bearing test and tensile test on laminate with and without a hole. The available experimental data in literature for different laminated composites were used to evaluate the joints strength. The agreement between experimental bearing strength for three different laminated composite plates evaluated and the analytically obtained joint strength by characteristic length method for each depends on the choice of failure criterion.

Table III: Predicted loads and the percentage difference between experimental values

Failure criteria	MO1 (kN)	MO2 (kN)	AS43501-6 (kN)	MO1 (%)	MO2 (%)	AS43501-6 (%)
Experi-ment	12.07	9.76	11.87	-	-	-
Yamada -Sun	11.40	10.40	14.20	-5.94	6.14	16.38
Azzi-Tsai	11.14	9.37	13.93	-8.35	-4.18	14.76
Norrs-Mckinnon	11.14	9.50	13.93	-8.35	-2.77	14.76
Norris	11.31	7.86	12.96	-6.73	-24.10	8.40
Fisher	11.40	6.92	11.89	-5.92	-41.06	0.20
Tsai-Wu	14.52	12.33	16.44	16.85	20.86	27.80
Average	11.81	9.40	13.89	-2.15	3.86	14.53

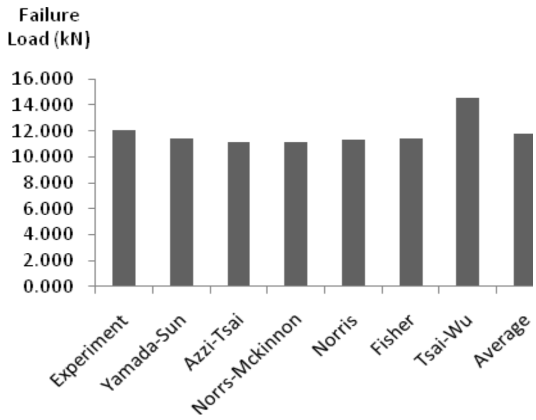

Fig. 6: Failure predictions for MO1 Plate, $[\pm45_3/90/\pm45_2/0_4/90/0_4//\pm45_2/90/\pm45_3]$

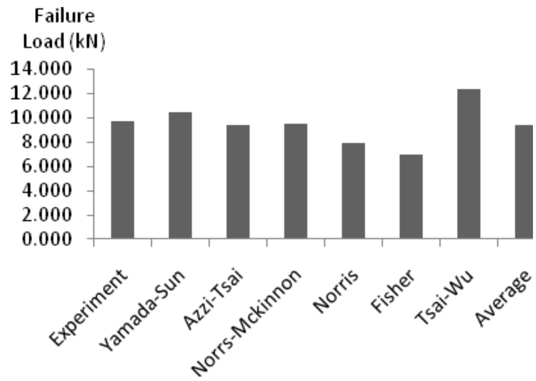

Fig.7: Failure predictions for MO2 plate, $[\pm45_3/90/\pm45_2/0_4/90/0_4//\pm45_2/90/\pm45_3]$

ISBN: 978-988-18210-7-2
ISSN: 2078-0958 (Print); ISSN: 2078-0966 (Online)

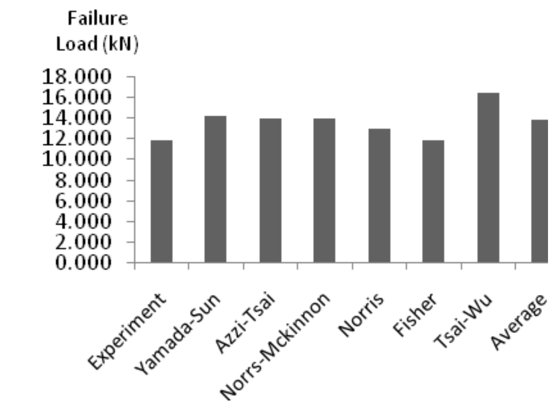

Fig. 8: Failure predictions for AS43501-6 Plate, $[(45/0/-45/0/90/0/45/0/-45/0)_2]_s$

There is no single failure criterion provided the best fit for all the plates evaluated; the average value of the predicted results from the six failure criteria investigated showed close agreement. Therefore, in order to optimize the accuracy of characteristic length method for joint strength prediction, three or more failure theories must be employed and an average calculated.

REFERENCES

[1] R.J. Nuismer, 1979, "Application of the average stress failure criterion: Part II - Compression," Journal of composite materials, 13, pp. 49-60.

[2] J.M. Whitney, and R.J. Nuismer, 1974, "Stress fracture criteria for laminated composites containing stress concentrations," Journal of composite materials, 8 (253), pp. 253-265.

[3] J.M. Whitney, and R.J. Nuismer, 1975, "Uniaxial failure of composite laminated containing stress concentrations," Fracture mechanics of composite, ASTM STP, pp. 117-142.

[4] F.K. Chang, and R.A. Scott, 1982, "Strength of mechanically fastened composite joints," Journal of composite materials, 16, pp. 470-494.

[5] J.T. Wang, C.G. Lotts, and D.D. Davis, Analysis of bolt-loaded elliptical holes in laminated composite joints. Journal of reinforced plastics and composites 1985;12: 128-138.

[6] Lekhnitskii, S.G., 1968, "Anisotropic plates", Translated from the 2nd Russian edition by S.W. Tsai, and T. Chevron, Gordon and Breach, London 1968.

[7] H. A. Whitworth, M. Othieno, and O. Barton, 2003, "Failure analysis of composite pin loaded joints," Composite structures, 59, pp. 261-266.

[8] H. A. Whitworth, O. Aluko, and N.A. Tomlinson, 2008, "Application of point stress criterion to the failure of composite pinned joints," Engineering fracture mechanics, 75, pp. 1829-1839.

[9] J. Kweon, H. Ahn, and J. Choi, 2004, "A new method to determine the characteristic lengths of composite joints without testing," Composite structures, 66, pp. 305-315.

[10] M.N. Nahas, 1986, "Survey of failure and post-failure theories of laminated fiber-reinforced composites," Journal of composites technology and research, 8(4), pp.138-153.

[11] J. Choi, and Y. Chun, 2003, "Failure load prediction of mechanically fastened composite joints," Journal of composite materials, 37(24), pp. 163-2177.

[12] O. Aluko, 2009, "Analytic determination of compressive characteristic length of composite plate," Early career journal, ASME 8, pp. 6.1-6.8.

[13] J.H. Konish, and J.M. Whitney, 1975, "Approximate stresses in an orthotropic plate containing a circular hole,"Journal of composite materials, 9, pp. 157-166.

[14] S.C. Tan, 1988, "Finite-width correction factors for anisotropic plate containing a central opening," Journal of composite materials, 22, pp.1080-1097.

[15] R.C. Burk, 1983, "Standard failure criteria needed for advanced composites," astronautics and aeronautics, 22, pp.58-62.

[16] M.J. Owen, and D.J. Rice, 1981, "Biaxial strength behavior of glass fabric-reinforced polyester resin," composites, 12, pp. 13-25.

ISBN: 978-988-18210-7-2
ISSN: 2078-0958 (Print); ISSN: 2078-0966 (Online)